SUPPLEMENTAL INFORMATION

Health and climate impacts of policy-driven changes in open crop straw burning during China's summer harvest

Jieyu Wen[a], Zhicheng Feng[a], Haochen Zuo[a], Xiaodong Xie[a], Ying Zhou[b,*], Yiyi Wang[c], Yang Hu[c], and Jianlin Hu[a,*]

[a] *Jiangsu Key Laboratory of Atmospheric Environment Monitoring and Pollution Control, Collaborative Innovation Center of Atmospheric Environment and Equipment Technology, School of Environmental Science and Engineering, Nanjing University of Information Science & Technology, Nanjing, 210044, China*

[b] *Key Laboratory of Beijing on Regional Air Pollution Control, College of Environment Science and Engineering, Beijing University of Technology, Beijing, 100124, China*

[c] *School of Energy and Environment, Anhui University of Technology, Ma'anshan 243000, China*

*Corresponding authors:

Dr. Jianlin Hu: jianlinhu@nuist.edu.cn

Dr. Ying Zhou: y.zhou@bjut.edu.cn

The supporting information includes 16 pages, 1 text, 9 figures, and 4 tables.

Text S1. Evaluation of WRF-Chem performance using surface meteorological and air-quality observations

We evaluated the model performance for meteorological variables in 2018 and 2021 (Fig. S4). Specifically, simulated 2 m air temperature (T_2), 2 m relative humidity (RH), and 10 m wind speed (WS) are generally consistent with observations. For T_2, the mean bias (MB), mean absolute error (MAE), and index of agreement (IOA) are −0.37, 1.43, and 0.94 in 2018. In 2021, the corresponding values are −0.41, 1.63, and 0.92. For RH, the IOA is 0.89 in 2018 and 0.88 in 2021. For WS, MB, MAE, root-mean-square error (RMSE), and IOA are 0.12, 0.91, 1.19, and 0.77 in 2018 and 0.08, 0.87, 1.13, and 0.76 in 2021, respectively. All statistics satisfy the performance goals recommended by Emery et al.[1] (T_2: MB ≤ ±0.50, MAE ≤ 2, IOA ≥ 0.80; RH: IOA ≥ 0.60; WS: MB ≤ ±0.50, MAE ≤ 2, RMSE ≤ 2, IOA ≥ 0.60). These results indicate that the model reasonably represents near-surface meteorological conditions over mainland China, supporting the quantification of OCSB impacts on air quality.

We also assessed model performance for $PM_{2.5}$, maximum daily 8-hour average ozone (MDA8 O_3), nitrogen dioxide (NO_2), and sulfur dioxide (SO_2) for 2013, 2018, and 2021 (Figs. S5–S6). For $PM_{2.5}$, normalized mean bias (NMB) is −10%, −5%, and 22% in 2013, 2018, and 2021, with normalized mean errors (NME) of 43%, 43%, and 52%, and correlation coefficients (R) of 0.66, 0.59, and 0.54, respectively. These metrics meet the criteria recommended by Emery et al.[2] (NMB ≤ ±30%, NME ≤ 50%, R > 0.40) in 2013 and 2018, with the 2021 NME still close to the 50% benchmark. For MDA8 O_3, the evaluation indicates a systematic underestimation, particularly in 2018 and 2021 (NMB = −30% and −24%), while the overall correlation with observations remains reasonable (R = 0.74 in both years). In addition, spatial comparisons further indicate that the model captures the main observed regional patterns of surface concentrations of key pollutants, including the contrast between heavily polluted areas (such as the North China Plain and adjacent regions) and relatively clean regions. Overall, the simulations show acceptable performance in reproducing both meteorology and key pollutant concentrations over mainland China, supporting the subsequent quantification of OCSB impacts.

Table S1. Model configurations of WRF-Chem.

Items	WRF-Chem	References
Micro Physics	The Purdue Lin	(Chen et al, 2002)[3]
Planetary Boundary Layer	The Yonsei University Scheme (YSU)	(Hong et al, 2006)[4]
Cumulus Parameterization	Grell 3D	(Grell et al, 2002)[5]
Shortwave radiation	RRTMG	(Iacono et al, 2008)[6]
Longwave radiation	RRTMG	(Iacono et al, 2008)[6]
Land surface	Noah	(Tewari et al, 2004)[7]
Surface Layer	Revised MM5	(Jimenez et al, 2012)[8]
Gas-phase chemistry	Carbon-Bond Mechanism version Z (CBMZ)	(Zaveri et al, 1999)[9]
Aerosol module	the 8-bin version of the Model for Simulating Aerosol Interactions and Chemistry (MOSAIC)	(Zaveri et al, 2008)[10]

Table S2. The statistical metrics and corresponding calculation formulas used in this study.

Statistical metric (abbrev.)	**Formula[a]**
Mean bias (MB)	$\frac{1}{N}\sum_{i=1}^{N}(P_i - O_i)$
Mean absolute error (MAE)	$\frac{1}{N}\sum_{i=1}^{N}\lvert P_i - O_i\rvert$
Root-mean-square error (RMSE)	$\left[\frac{1}{N}\sum_{i=1}^{N}(P_i - O_i)^2\right]^{\frac{1}{2}}$
Index of agreement (IOA)	$1 - \frac{\sum_{i=1}^{N}(P_i - O_i)^2}{\sum_{i=1}^{N}(\lvert P_i - \bar{O}\rvert + \lvert O_i - \bar{O}\rvert)^2}$
Normalized mean bias (NMB)	$\frac{\sum_{i=1}^{N}(P_i - O_i)}{\sum_{i=1}^{N} O_i} \times 100\%$
Normalized mean error (NME)	$\frac{\sum_{i=1}^{N}\lvert P_i - O_i\rvert}{\sum_{i=1}^{N} O_i} \times 100\%$
Correlation coefficient (R)	$\frac{\sum_{i=1}^{N}(P_i - \bar{P})(O_i - \bar{O})}{\sqrt{\sum_{i=1}^{N}(P_i - \bar{P})^2}\sqrt{\sum_{i=1}^{N}(O_i - \bar{O})^2}}$

[a]In the equations, P_i denotes the model-predicted (simulated) value and O_i the observed value. N is the number of paired samples, and i indexes the ith pair ($i = 1, \cdots, N$). $\bar{P}$ and $\bar{O}$ are the sample means of the predicted and observed values, respectively.

Table S3. The 74 major cities used for model evaluation.

Region	City lists
Northeast China (4)	1. Shenyang, 2. Dalian, 3. Changchun, 4. Harbin
North China (15)	5. Beijing, 6. Tianjin, 7. Shijiazhuang, 8. Tangshan, 9. Qinhuangdao, 10. Handan, 11. Xingtai, 12. Baoding, 13. Zhangjiakou, 14. Chengde, 15. Cangzhou, 16. Langfang, 17. Hengshui, 18. Taiyuan, 19. Hohhot
Central China (4)	20. Hefei, 21. Nanchang, 22. Zhengzhou, 23. Wuhan
East China (29)	24. Shanghai, 25. Nanjing, 26. Wuxi, 27. Xuzhou, 28. Changzhou, 29. Suzhou, 30. Nantong, 31. Lianyungang, 32. Huai'an, 33. Yancheng, 34. Yangzhou, 35. Zhenjiang, 36. Taizhou (Jiangsu), 37. Suqian, 38. Hangzhou, 39. Ningbo, 40. Wenzhou, 41. Jiaxing, 42. Huzhou, 43. Shaoxing, 44. Jinhua, 45. Quzhou, 46. Zhoushan, 47. Taizhou (Zhejiang), 48. Lishui, 49. Fuzhou, 50. Xiamen, 51. Jinan, 52. Qingdao
South China (12)	53. Changsha, 54. Guangzhou, 55. Shenzhen, 56. Zhuhai, 57. Foshan, 58. Jiangmen, 59. Zhaoqing, 60. Huizhou, 61. Dongguan, 62. Zhongshan, 63. Nanning, 64. Haikou
Southwest China (5)	65. Chongqing, 66. Chengdu, 67. Guiyang, 68. Kunming, 69. Lhasa
Northwest China (5)	70. Xi'an, 71. Lanzhou, 72. Xining, 73. Yinchuan, 74. Ürümqi

Table S4. Definition of four analysis regions and province lists.

Region	Provinces
North China	Beijing, Tianjin, Hebei, Shanxi, Inner Mongolia
East China	Shanghai, Jiangsu, Zhejiang, Anhui, Fujian, Jiangxi, Shandong
Central China	Henan, Hubei, Hunan
Northeast China	Liaoning, Jilin, Heilongjiang

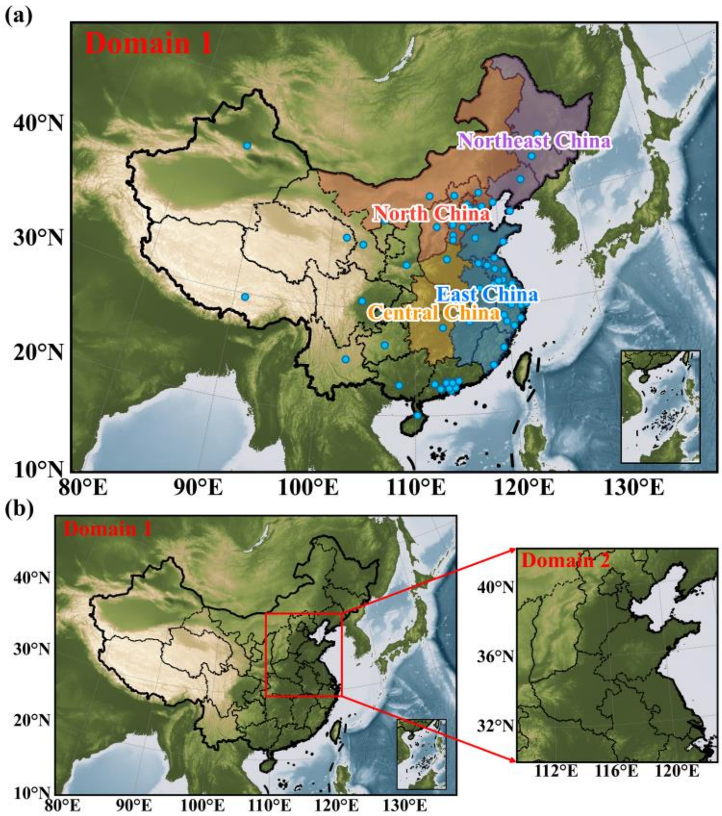

Fig. S1 WRF-Chem modeling configuration and evaluation sites. (a) Four key analysis regions (Northeast China, North China, East China, and Central China) and the 74 cities used for model evaluation (Table S3; blue dots denote evaluation sites). (b) Outer (Domain 1) and nested (Domain 2) WRF-Chem domains covering China and the North China Plain.

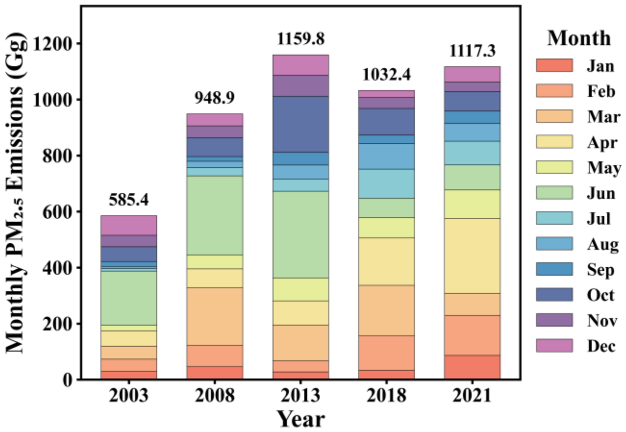

Fig. S2 Monthly OCSB-induced $PM_{2.5}$ emissions over mainland China for 2003, 2008, 2013, 2018 and 2021.

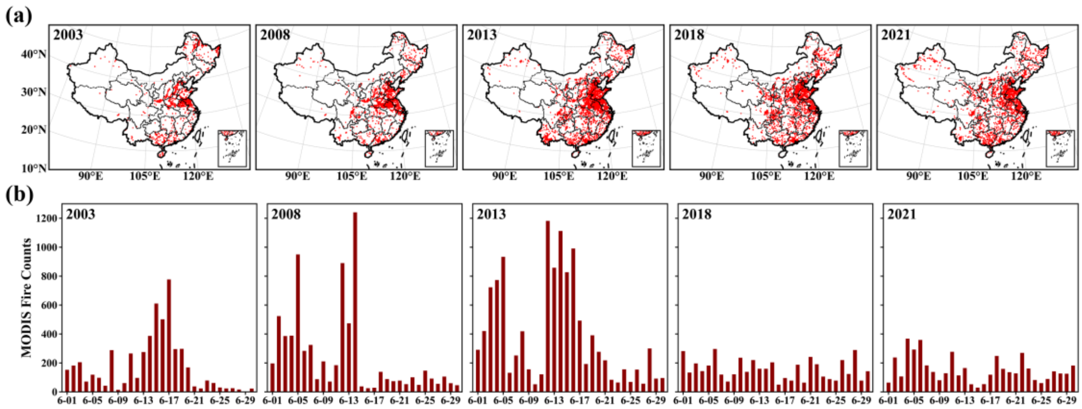

Fig. S3 Spatial distribution (a) and daily counts (b) of MODIS active-fire detections for June 2003, 2008, 2013, 2018, and 2021 across mainland China.

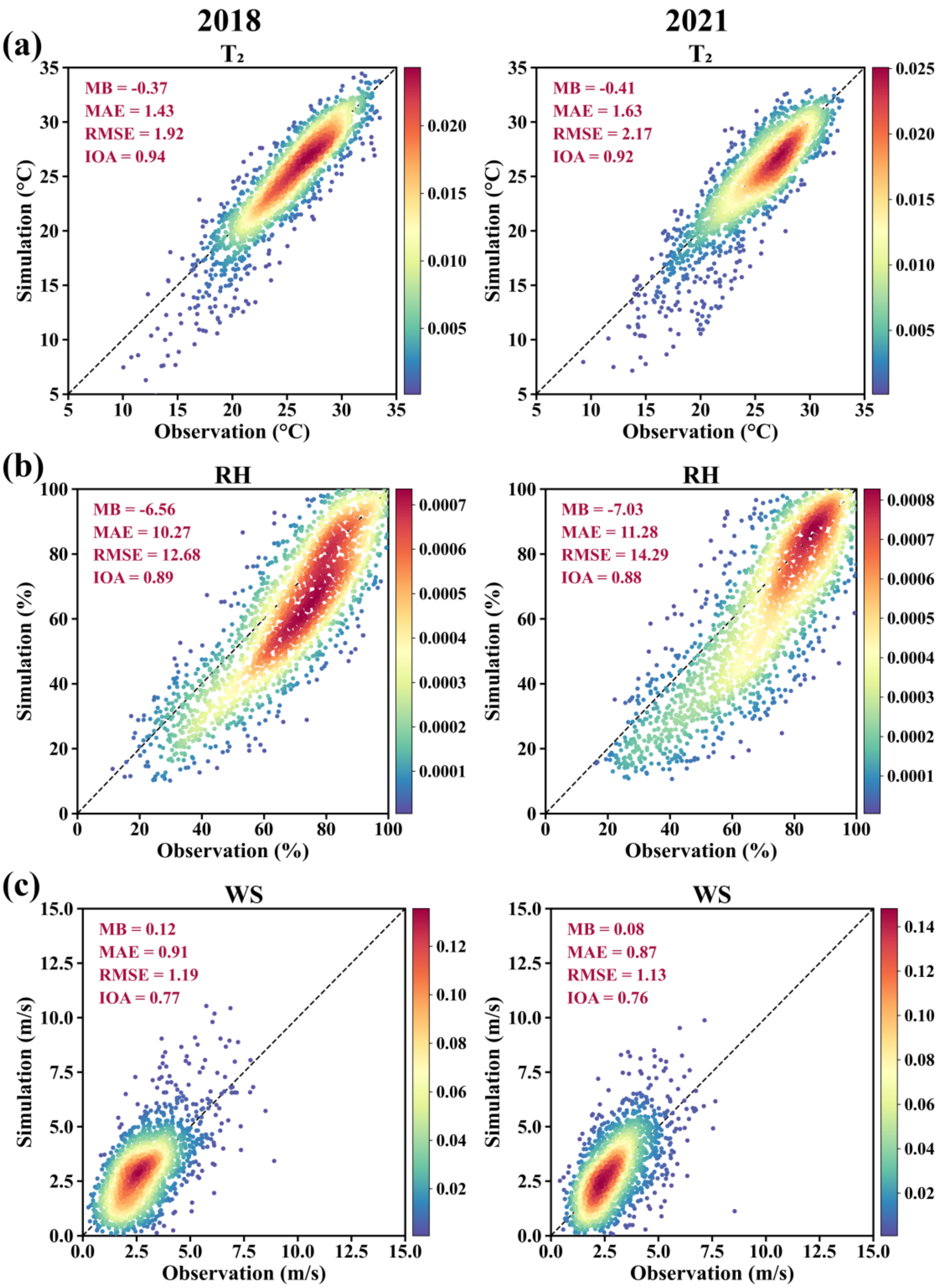

Fig. S4 Evaluation of T_2, RH, and WS against observations for June 2018 (left) and June 2021 (right) across 74 cities. (*Colors show point density; the dashed line is 1:1.*)

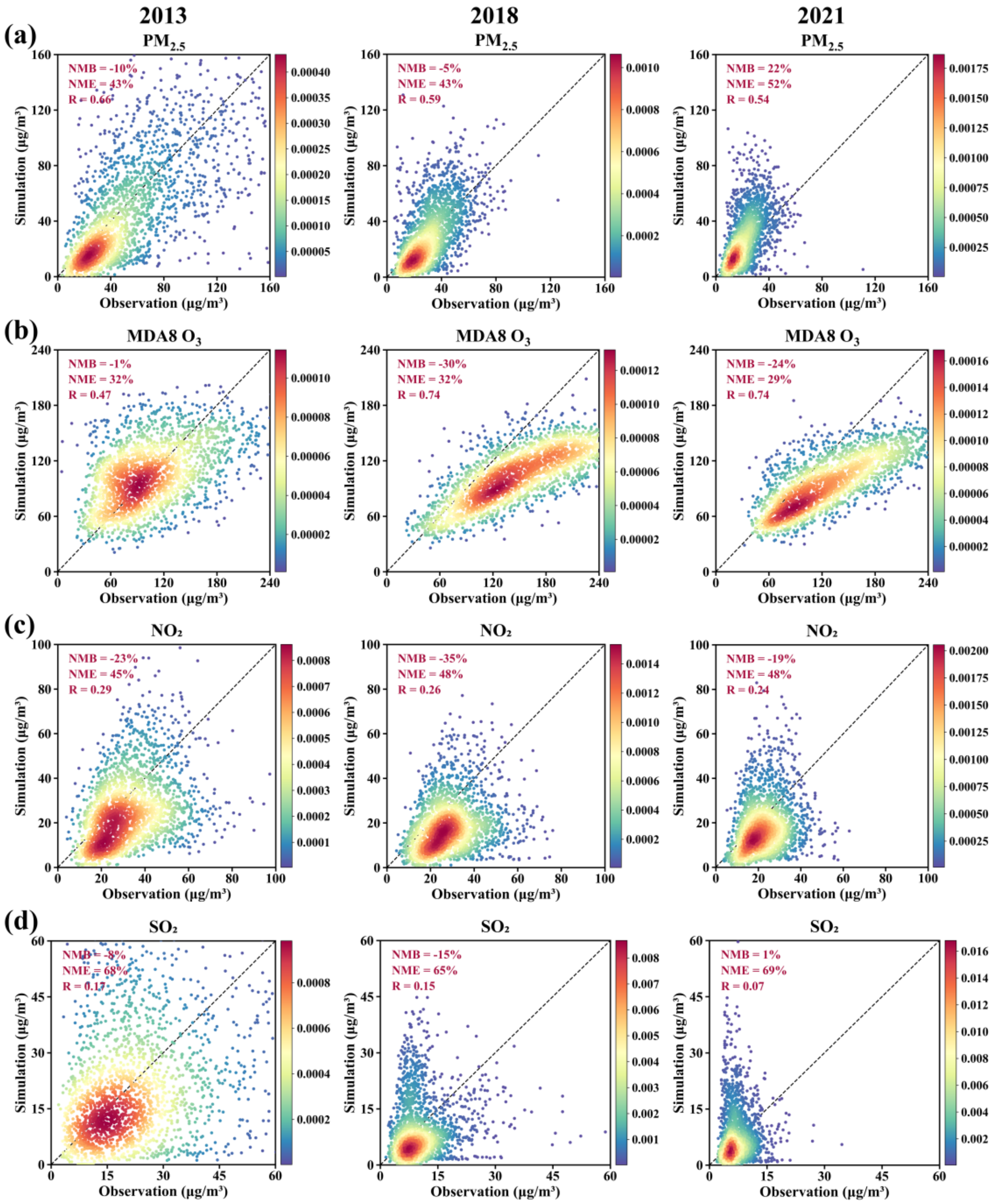

Fig. S5 Evaluation of $PM_{2.5}$, MDA8 O_3, NO_2, and SO_2 against observations for June 2013 (left), 2018 (middle), and 2021 (right) across 74 cities. (*Colors show point density; the dashed line is 1:1.*)

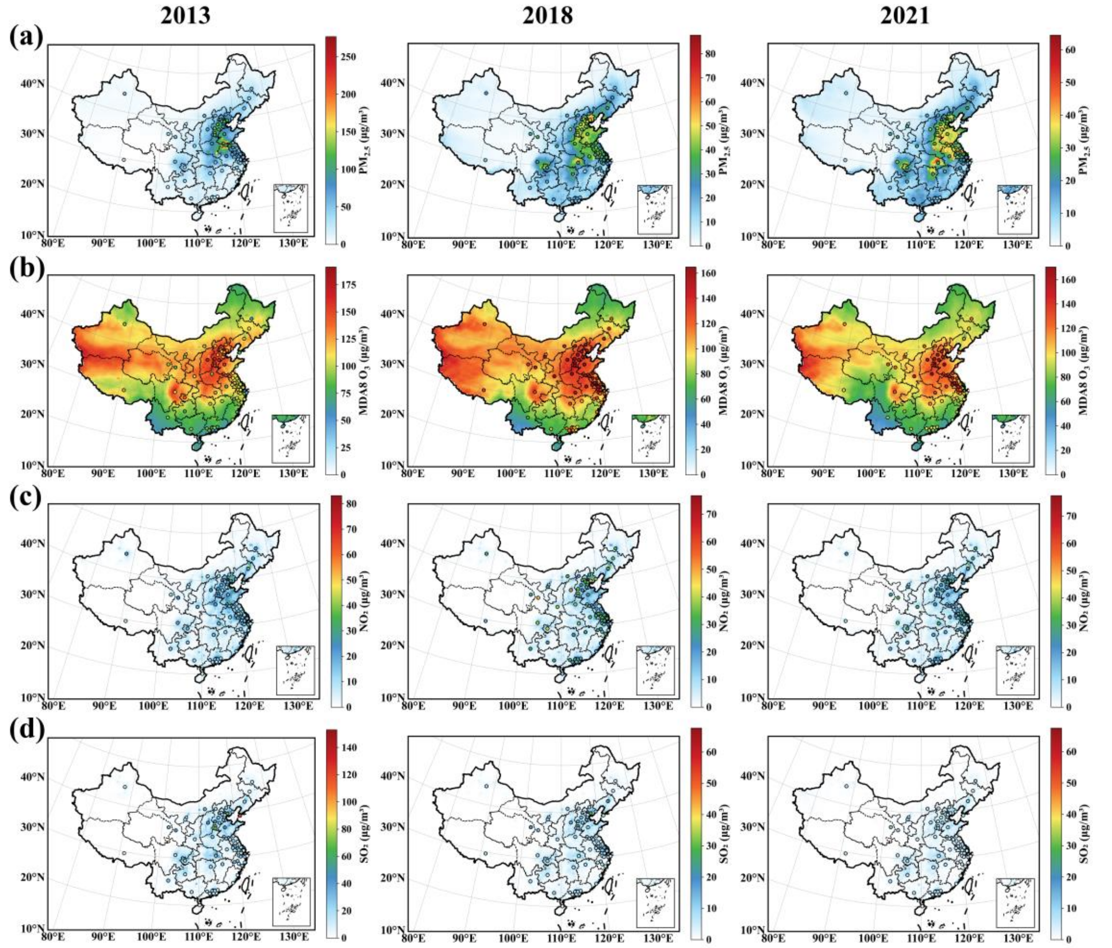

Fig. S6 Spatial evaluation of $PM_{2.5}$, MDA8 O_3, NO_2, and SO_2 across mainland China for June 2013 (left), 2018 (middle), and 2021 (right). (*Dots denote observed concentrations at city sites.*)

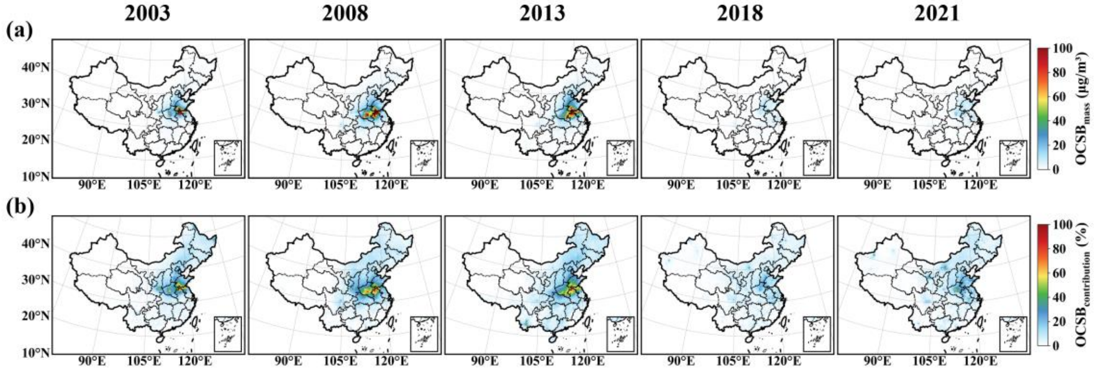

Fig. S7 Contribution of open crop straw burning (OCSB) to $PM_{2.5}$ mass concentration across mainland China for June 2003, 2008, 2013, 2018, and 2021. (a) absolute concentration (μg/m^3); (b) relative contribution (%).

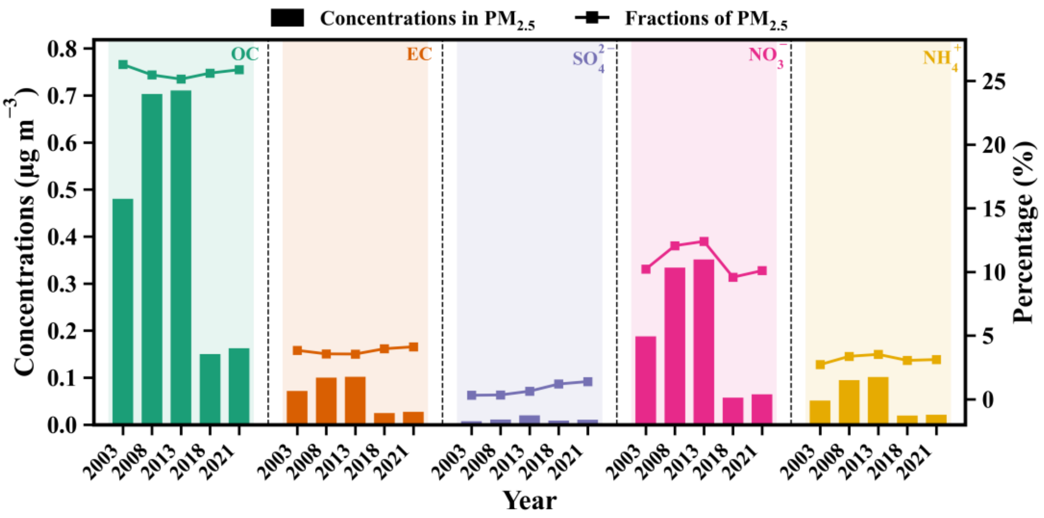

Fig. S8 Absolute concentrations (bars, left axis) and fractions (lines, right axis) of major $PM_{2.5}$ components within OCSB-attributable $PM_{2.5}$ in June for 2003, 2008, 2013, 2018, and 2021.

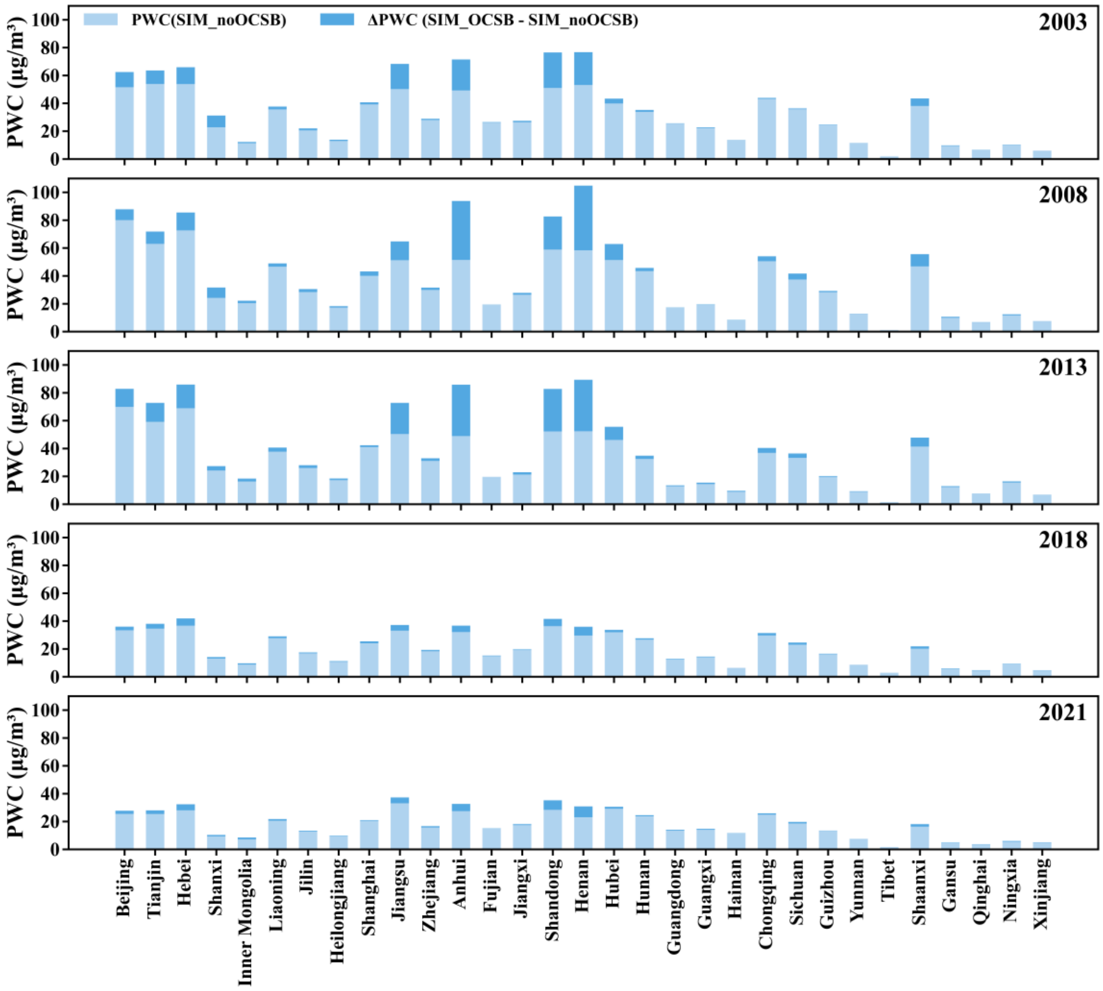

Fig. S9 Population-weighted $PM_{2.5}$ concentration (PWC) across 31 provinces of mainland China for June 2003, 2008, 2013, 2018, and 2021.

References

1 C. Emery, E. Tai and G. Yarwood, Enhanced meteorological modeling and performance evaluation for two Texas ozone episodes, Prepared for the Texas natural resource conservation commission, by ENVIRON International Corporation, 2001, **161**.

2 C. Emery, Z. Liu, A. G. Russell, M. T. Odman, G. Yarwood and N. Kumar, Recommendations on statistics and benchmarks to assess photochemical model performance, Journal of the Air & Waste Management Association, 2017, **67**, 582-598.

3 S. H. Chen and W. Y. Sun, A one-dimensional time dependent cloud model, Journal of the Meteorological Society of Japan, 2002, **80**, 99-118.

4 S.-Y. Hong, Y. Noh and J. Dudhia, A new vertical diffusion package with an explicit treatment of entrainment processes, Monthly Weather Review, 2006, **134**, 2318-2341.

5 G. A. Grell, Prognostic evaluation of assumptions used by cumulus parameterizations, Monthly weather review, 1993, **121**, 764-787.

6 M. J. Iacono, J. S. Delamere, E. J. Mlawer, M. W. Shephard, S. A. Clough and W. D. Collins, Radiative forcing by long - lived greenhouse gases: Calculations with the AER radiative transfer models, Journal of Geophysical Research: Atmospheres, 2008, **113**.

7 M. Tewari, Implementation and verification of the unified NOAH land surface model in the WRF model, In 20th Conference on Weather Analysis and Forecasting/16th Conference on Numerical Weather Prediction; AMS: Seattle, WA, USA, 2004, **Vol. 14.2A**, pp 11−15.

8 P. A. Jiménez, J. Dudhia, J. F. González-Rouco, J. Navarro, J. P. Montávez and E. García-Bustamante, A revised scheme for the WRF surface layer formulation, Monthly weather review, 2012, **140**, 898-918.

9 R. A. Zaveri and L. K. Peters, A new lumped structure photochemical mechanism for large - scale applications, Journal of Geophysical Research: Atmospheres, 1999, **104**, 30387-30415.

10 R. A. Zaveri, R. C. Easter, J. D. Fast and L. K. Peters, Model for Simulating Aerosol Interactions and Chemistry (MOSAIC), Journal of Geophysical Research: Atmospheres, 2008, **113**.